International Journal on Recent and Innovation Trends in Computing and Communication
ISSN: 2321-8169 Volume: 11 Issue: 4s
DOI: https://doi.org/10.17762/ijritcc.v11i4s.6319
***Article Received**: 22 December 2022 **Revised**: 30 January 2023 **Accepted**: 12 February 2023*

Interpolation of Low-Resolution Images for Improved Accuracy Using an ANN Quadratic Interpolator

Diana Earshia V*, Sumathi M[2]
*****Research Scholar, Department of Electronics and Communication Engineering
Sathyabama Institute of Science and Technology
Chennai, India
earshy@gmail.com
*****Assistant Professor, Department of Electronics and Communication Engineering,
Vel Tech Rangarajan Dr Sagunthala R&D Institute of Science and Technology
Chennai, Tamilnadu 600062, India
[2]Professor, Department of Electronics and Communication Engineering
Sathyabama Institute of Science and Technology
Chennai, India
Sumagopi206@gmail.com

Abstract—The era of digital imaging has transitioned into a new one. Conversion to real-time, high-resolution images is considered vital. Interpolation is employed in order to increase the number of pixels per image, thereby enhancing spatial resolution. Interpolation's real advantage is that it can be deployed on user end devices. Despite raising the number of pixels per inch to enhances the spatial resolution, it may not improve the image's clarity, hence diminishing its quality. This strategy is designed to increase image quality by enhancing image sharpness and spatial resolution simultaneously. Proposed is an Artificial Neural Network (ANN) Quadratic Interpolator for interpolating 3-D images. This method applies Lagrange interpolating polynomial and Lagrange interpolating basis function to the parameter space using a deep neural network. The degree of the polynomial is determined by the frequency of gradient orientation events within the region of interest. By manipulating interpolation coefficients, images can be upscaled and enhanced. By mapping between low- and high-resolution images, the ANN quadratic interpolator optimizes the loss function. ANN Quadratic interpolator does a good work of reducing the amount of image artefacts that occur during the process of interpolation. The weights of the proposed ANN Quadratic interpolator are seeded by transfer learning, and the layers are trained, validated, and evaluated using a standard dataset. The proposed method outperforms a variety of cutting-edge picture interpolation algorithms..

Keywords- ANN; Image Interpolation; Lagrange polynomial; Deep learning; Lagrange basis function; Quadratic Interpolation.

I. INTRODUCTION

The human visual system recognizes spatial resolution as an essential feature. Enhancing spatial resolution is done by increasing the number of pixels per image. Images with inadequate resolution require correction. These low-resolution images are a result of the sensitivity of the camera device, the significant distance between the target and the camera, image compression, etc. Interpolation is possible with medical images, satellite photos, digital photographs, surveillance images, astronomical images, and game visuals [1]. Interpolation contributes to the enhancement of an image's spatial resolution. The impact of image resolution improvement relies on the end device, the requirements, and the application. Self-Adaptive rapid interpolating is a necessity for modern applications [2]. [3]. Deep CNN demonstrates promising results for image restoration, scaling, creation, and transformation. Super-resolution models trained with mean-square-error (MSE) loss tend to provide overly smooth pictures [4]. For image restoration, generative adversarial networks (GAN) generate images with some undesirable noise [5].

A higher spatial resolution results in a more accurate depiction of intricate structures. High resolution photos contain approximations of information derived from existing pixels, but no new information [6]. There must be a compromise, as an image with an increase in information may not be aesthetically pleasing. Low interpolation error can be achieved with prior knowledge of the source image and judicious technique choice. As Interpolation can be integrated as part of a subsystem's design, the computational cost is diminished [7]. Reconstructing high frequency components in images presents significant technical problems. Reconstructing high-resolution

International Journal on Recent and Innovation Trends in Computing and Communication
ISSN: 2321-8169 Volume: 11 Issue: 4s
DOI: https://doi.org/10.17762/ijritcc.v11i4s.6319
***Article Received**: 22 December 2022 **Revised**: 30 January 2023 **Accepted**: 12 February 2023*

images from the same set of pixels is impossible. Minor inaccuracies around edges and textures have a significant effect on visual quality since HVS is extremely sensitive to edges and textures. When multidimensional images are to be interpolated, they must be divided into various channels and then further processed. Obtaining interpolated images with a high resolution becomes more complicated and time-consuming as the dimensions are expanded. The resulting high-resolution images must be devoid of image abnormalities including jagging, blurring, halos, and blocking.

The best method for obtaining high-resolution photos is an artificial neural network [8]. In order to generate new pixels in the spatial domain, parameters are shared on the same space. Deep Neural Networks do not require a separate module for dimensionality reduction, hence solving the curse of dimensionality, because the model learns compact representations inside itself.

.

II. RELATED WORKS

Aguerrebere et al. (2017) [9] discuss the computation of missing pixels in digital photography using a signal-dependent noise model. The author achieves success by employing a Hyperprior Bayesian estimator to stabilise the local estimation, hence increasing the precision of local model estimation for normal restoration issues. It is limited by the kernel problem encountered during deconvolution.

Authors Tikhonov et al. (2014) [10] proposed an algebraic representation of geometric similarities, gradient-based directional regularisation, and a library of matched reference picture patches. Measurement of similarity based on Euclidean distance, scaled Euclidean distance, and non-local searching for matched picture patches. This approach requires a minimum of four reference photos from matched photographs for processing.

Niknejad et al. (2015) [11] describe a picture interpolation model based on Gaussian Mixture. This neighborhood's related patches are estimated using a multivariate Gaussian probability function. The manipulation of the weights of Gaussian distributions in an aggregative manner results in complex calculations requiring additional memory and time.

Noor et al. (2019) [12] propose a technique that generates DoG images from two distinct input scenarios and subtracts them to obtain residual value, which is then used to train a deep learning network to produce high-resolution images that preserve SIFT repeatability. Finding the suitable sigma values in Gaussian filter is problematic, making the procedure difficult.

Chitra et al. (2020) [13] offer a unique method for selecting satellite image interpolation patches utilising fuzzy logic and ANN B-splines. The image is segmented into patches, which are then processed. Additional processing time, greater than one second, is necessary to get a satellite image with a high resolution. It also necessitates the modification of hardware requirements to reduce processing time.

Vijay et al. (2011) [14] provided a framework to calculate low bit-rate feature descriptors with a 20 reduction in bit rate; this framework was deployed in a mobile retrieval system with a 96% accuracy rate. This strategy boosts spatial resolution but disregards image quality. In addition, the images utilised were CD and book covers, whose sizes are much less than 256 by 256 images.

Sivaram prasad et al. (2018) [15] offer a method for identifying a high quality image from a low resolution image utilizing two CNN channels. Here, low-resolution and high-resolution image sets are input to a CNN with two channels. This approach requires both low-resolution and high-resolution image sets as input. Without this, scaling cannot be performed.

Kim et al. (2016) [1]utilized a deep CNN, VDSR, for ImageNet categorization. The low-resolution image is combined with the residual image to produce a high-resolution image. A reference image with a high resolution is required to obtain a residual image. No reference image cannot be upscaled using this method.

Bee man et al. (2017) [16]added residual blocks with a scale factor of 0.1 to the CNN design. This consolidated the training process. In this architecture, the depth of the convolution layer is raised, which enhances the network's complexity.

Deep Network Interpolation (DNI) is a technique proposed by Xintao Wang et al. (2019) [17] that applies linear interpolation to the parameter space of two or more linked networks. By fine-tuning the interpolation coefficients, he achieves a smooth control of picture effects in his suggested network. This is effective for style transfer between photographs, but fails to preserve the image's quality and individuality.

Chao Dong et al. (2016) proposes a deep learning technique for single image super-resolution[18], its further proven that classic sparse-coding-based SR methods may be considered as a deep convolutional network to convert low resolution image to high resolution image. Effective high-resolution photographs with varying scaling factors is a question.

International Journal on Recent and Innovation Trends in Computing and Communication
ISSN: 2321-8169 Volume: 11 Issue: 4s
DOI: https://doi.org/10.17762/ijritcc.v11i4s.6319
***Article Received**: 22 December 2022 **Revised**: 30 January 2023 **Accepted**: 12 February 2023*

In this paper, a novel methodology is proposed with the goals of overcoming the limits posed by the demand of high-resolution reference images, conserving and improving the quality of upscaled images, reducing the complexity of dense designs, and shortening the amount of time required for the processing of images.

III. PROPOSED METHOD

Figure 1 demonstrates the proposed method for getting a high-resolution image from a low-resolution image using an ANN Quadratic interpolator. High-resolution image databases provide the ground truth images, also known as High-resolution photos.

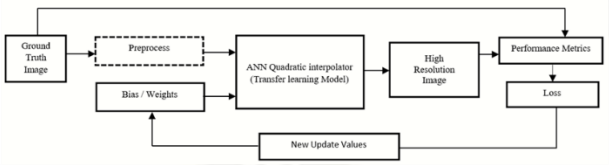

Figure 1. Block Diagram of Proposed Method

The ANN Quadratic interpolator is trained using images from three different picture datasets. As training data for ANN Quadratic interpolator, ground truth pictures from the three datasets IAPR TC-12, DIV2K, and CDVS are used. IAPR TC-12 contains 20,000 still natural images, whereas DIV 2K contains 1,000 images and CDVS contains 186K annotated images. Table 1 provides few sample of the images present in the considered datasets.

TABLE I. IMAGE SAMPLES FROM DATASETS

Data set	No of images	Images samples from datasets
IAPR TC-12 [19]	20,000 still natural images	
DIV 2K [20]	1000 train images images	
CDVS [21]	186k labeled images	

Compatible with VGG [22] and ResNet [23] is the proposed ANN Quadratic interpolator. The input photos are downsized to 224x224x3 in the preprocessing phase. These photos are sampled at half their original resolution. These down sampled images are considered low-resolution images and are fed to the interpolation process. ANN Quadratic interpolator is fed these Low-Quality pictures.

Resnet50 architecture is modified in order to create an ANN Quadratic interpolator. The architecture of the skip network facilitates a quicker weight update during back propagation. The weights are transfer learned from ImageNet dataset training. The final layer of the ResNet50 architecture is adjusted to provide a single interpolated value that has been processed. By increasing the number of hidden layers and the number of neurons per layer, it is possible to expand the depth and width of an architecture. After each residual block is max pooling, the same padding, and the ReLu activation function. In the parameter space, the convolutional layers employ the Lagrange interpolating polynomial and its basis function. CNN shares parameters geographically and does internal dimension reduction. The adaptive tweaking of Lagrange interpolating coefficients improves the spatial resolution of input images of poor resolution.

$$P_L(x,y) = y_0\, L_0(x,y) + y_1\, L_1(x,y) + y_2\, L_2(x,y) \quad (1)$$

where,

$$L_0(x,y) = \frac{(x-x_1)(x-x_2)}{(x_0-x_1)(x_0-x_2)} * \frac{(y-y_1)(y-y_2)}{(y_0-y_1)(y_0-y_2)} \quad (1a)$$

$$L_1(x,y) = \frac{(x-x_0)(x-x_2)}{(x_1-x_0)(x_1-x_2)} * \frac{(y-y_0)(y-y_2)}{(y_1-y_1)(y_1-y_2)} \quad (1b)$$

$$L_2(x,y) = \frac{(x-x_0)(x-x_1)}{(x_2-x_0)(x_2-x_1)} * \frac{(y-y_0)(y-y_1)}{(y_2-y_0)(y_2-y_1)} \quad (1c)$$

* is convolution function

Equation (1) is the quadratic Lagrange interpolating polynomial and $L_0(x,y)$, $L_1(x,y)$, $L_2(x,y)$ are the Lagrange's interpolating basis functions, which are given in equations 1a to 1c. The degree of polynomial is based on the event occurrences of gradient orientation in the region of interest. The gradients $\frac{\partial P_L}{\partial x}, \frac{\partial P_L}{\partial y}$ are calculated using convolve filters with image. Its magnitude is manipulated by norm function

$$||\nabla P_L|| = \sqrt{\left(\frac{\partial P_L}{\partial x}\right)^2 + \left(\frac{\partial P_L}{\partial y}\right)^2} \quad (2)$$

and its orientation is manipulated as

$$\theta = tan^{-1}\left(\frac{\frac{\partial P_L}{\partial x}}{\frac{\partial P_L}{\partial y}}\right) \quad (3)$$

A few upscaling techniques may result in fuzzy photos that lack fine details. When upscaling low-resolution photos, it is occasionally impossible to remove faults or compression artifacts. They can be repaired using the ANN Quadratic interpolator that has been proposed. Each convolutional layer of the ANN Quadratic interpolator collects many features, such as edges, corners, forms, textures, patterns, illumination, object components, and objects, etc. Feature is nonetheless a data transformation. For the purpose of updating weights, the SSIM-structural Similarity Index is utilized as either the loss function or the cost function. The stochastic gradient descent (SGD) algorithm is used to optimize the cost function by modifying trainable parameters iteratively. The new weight is calculated

International Journal on Recent and Innovation Trends in Computing and Communication
ISSN: 2321-8169 Volume: 11 Issue: 4s
DOI: https://doi.org/10.17762/ijritcc.v11i4s.6319
***Article Received**: 22 December 2022 **Revised**: 30 January 2023 **Accepted**: 12 February 2023*

as the product of learning rate and gradient minus the old weight. As L1 generalization, the mean absolute function is employed to prevent overfitting. Initial learning rate is set to 10^{-4}. Strong Correlation between convolutional layers gives images with a high PSNR value when interpolated.

Using a 6:2:2 ratio, the network is trained, validated, and tested. Validation dataset helps to fine tune hyperparameters to increase model performance. The performance of the model is evaluated using metrics such as Peak Signal to Noise Ratio (PSNR), Structural Similarity Index (SSIM), Edge Peak Signal to Noise Ratio (EPSNR), and Feature Similarity Index (FSIM).

IV. Results and Discussion

Jupyter notebook was employed for model training, validation, and testing. Figure 2 depicts the first layer of the ANN Quadratic interpolator for reference. The remaining blocks adhere to the same pattern. The interpolator's depth is enhanced by increasing the number of hidden layers. The residual structure enables the weights to be easily updated by back propagation, removing the influence of gradients that converge to zero.

Layer (type)	Output Shape	Param #	Connected to
input_2 (InputLayer)	[(None, None, None, 3)]	0	[]
conv1_pad (ZeroPadding2D)	(None, None, None, 3)	0	['input_2[0][0]']
conv1_conv (Conv2D)	(None, None, None, 64)	9472	['conv1_pad[0][0]']
conv1_bn (BatchNormalization)	(None, None, None, 64)	256	['conv1_conv[0][0]']
conv1_relu (Activation)	(None, None, None, 64)	0	['conv1_bn[0][0]']
pool1_pad (ZeroPadding2D)	(None, None, None, 64)	0	['conv1_relu[0][0]']
pool1_pool (MaxPooling2D)	(None, None, None, 64)	0	['pool1_pad[0][0]']

Figure 2. First layer of ANN Quadratic interpolator

The total number of parameters, trainable parameters and Non-trainable parameters are shown in figure 3

```
Total params: 25,691,013
Trainable params: 2,103,301
Non-trainable params: 23,587,712
```

Figure 3. Statistics of Parameters

In this section, the outcomes of the experiment are summarized and discussed. The ANN Quadratic interpolator is trained, validated, and tested using IAPR TC-12, DIV2K, and CDVS datasets. Bicubic interpolation, New Edge Interpolation (NEDI), Bayesian based hyperparameter interpolation (Bayesian), Edge deep super resolution (EDSR), Very deep super resolution (VDSR), Non geometric similarity directional gradient (NGSDG), Fuzzy logic ANN Bayesian hyperprior interpolation (FLABBHI) are the other interpolation techniques considered for comparison with proposed ANN Quadratic interpolator. PSNR, SSIM, EPSNR, and FSIM indicate how well the parameters or characteristics of an interpolated image match with the image that represents the ground truth.

4.1 Comparison of Interpolation results for few Benchmark Images

Images	Metrics	Bicubic	NEDI	Bayesian	EDSR	VDSR	NGSDG	FLABBHI	Proposed
Lena	PSNR	24.8248	27.1225	35.7554	35.5858	34.5899	30.8882	40.1018	43.0118
	SSIM	0.8737	0.8774	0.8797	0.8897	0.8997	0.8853	0.9097	0.9557
House	PSNR	23.8222	24.7256	33.1834	36.1252	37.5632	30.2413	40.3125	41.8315
	SSIM	0.8266	0.8671	0.8989	0.8899	0.8989	0.8669	0.9389	0.9556
Boats	PSNR	25.8348	27.1235	26.7534	36.5828	35.5899	31.8822	41.1718	44.0418
	SSIM	0.8758	0.8775	0.8691	0.8891	0.8991	0.8876	0.9288	0.9565
Mandrill	PSNR	27.1923	33.7449	34.8245	34.7465	37.7834	39.4793	35.2246	41.6872
	SSIM	0.8571	0.8731	0.8887	0.8887	0.8897	0.8563	0.9387	0.9567
Peppers	PSNR	27.2445	28.4563	32.3223	35.7427	36.5524	31.2001	38.8472	41.4172
	SSIM	0.8718	0.8766	0.8866	0.8896	0.8986	0.8878	0.9186	0.9641
Average	**PSNR**	**25.7837**	**28.2346**	**32.5678**	**35.7566**	**36.4158**	**32.7382**	**39.1316**	**42.3979**
	SSIM	**0.8610**	**0.8743**	**0.8846**	**0.8894**	**0.8972**	**0.8768**	**0.9269**	**0.9577**

The following graphs, shown in figure 4a and figure 4b, presents a comparison of the existing and suggested interpolators with regard to the average outcomes of PSNR and SSIM. The ANN interpolator that was proposed has a PSNR average value of 42.3979, and its SSIM average value is 0.9577, which is higher than the other techniques that are currently in use.

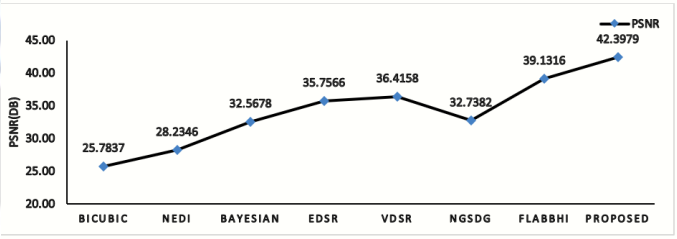

Figure 4a. PSNR values of few bench mark images using proposed and existing algorithms

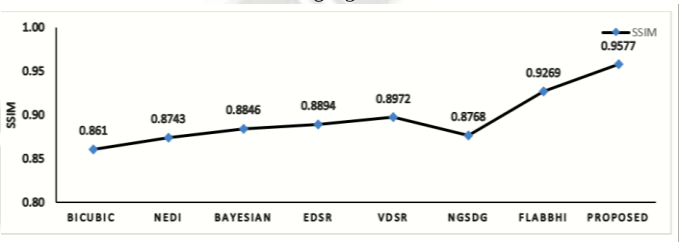

Figure 4b. SSIM values of few bench mark images using proposed and existing algorithms

International Journal on Recent and Innovation Trends in Computing and Communication
ISSN: 2321-8169 Volume: 11 Issue: 4s
DOI: https://doi.org/10.17762/ijritcc.v11i4s.6319
***Article Received**: 22 December 2022 **Revised**: 30 January 2023 **Accepted**: 12 February 2023*

4.2 Comparison of Interpolation results using Datasets

The performance evaluation of a number of different interpolation methods is compared with proposed ANN interpolator in table 3, and the graphical charts associated with those approaches are presented further below. IAPR TC-12, DIV 2K, and CVDS are the three datasets that are used for the training, validation, and testing phases of this comparative study. The values that are displayed in the table represent the average values of the metrics PSNR, SSIM, EPSNR, and FSIM.

Figure 5a, figure 5b, figure 5c and figure 5d, displays a comparison of the recommended and current interpolators with relation to the average results of PSNR, SSIM, EPSNR, and FSIM. The following figures exhibit this comparison. The ANN interpolator that was suggested has higher values than the other methods that are currently being utilized. Its PSNR average value is 40.3979, its SSIM average value is 0.9554, its EPSNR average value is 34.3329, and its FSIM average value is 0.9883. These values are all higher than the averages of the other techniques.

Dataset	Metrics	Different Interpolation methods							
		Bicubic	*NEDI*	*Bayesian*	*EDSR*	*VDSR*	*NGSDG*	*FLABBHI*	*Proposed*
Dataset 1 (IAPR TC-12)	PSNR	25.6103	26.8241	33.7215	34.9217	35.9791	31.4567	38.5760	40.9742
	SSIM	0.8652	0.8713	0.8797	0.8888	0.8981	0.8760	0.9329	0.9563
	EPSNR	18.5581	31.4867	24.9936	32.7631	33.2624	21.7457	31.6165	34.2209
	FSIM	0.8934	0.9470	0.9389	0.9510	0.9829	0.9296	0.9762	0.9882
Dataset 2 (DIV 2K)	PSNR	25.2597	25.9624	32.8755	34.2185	34.9031	30.3813	37.7080	40.0176
	SSIM	0.8585	0.8731	0.8685	0.8798	0.8966	0.8734	0.9283	0.9528
	EPSNR	18.5672	30.8264	24.9363	32.7520	33.2623	21.7530	31.4341	34.5275
	FSIM	0.8934	0.9470	0.9389	0.9510	0.9829	0.9296	0.9762	0.9882
Dataset 3 (CDVS)	PSNR	26.7160	27.8976	34.3080	35.8602	36.5802	32.3391	39.3406	41.8392
	SSIM	0.8648	0.8814	0.8982	0.9024	0.8874	0.9074	0.9475	0.9571
	EPSNR	18.6970	31.5498	25.0031	32.7701	33.2726	21.7503	31.7308	34.2503
	FSIM	0.8867	0.9458	0.9365	0.9466	0.9838	0.9308	0.9768	0.9885
Average	**PSNR**	**25.9879**	**26.9300**	**33.5918**	**35.0394**	**35.7417**	**31.3602**	**38.5243**	**40.9284**
	SSIM	**0.8628**	**0.8753**	**0.8821**	**0.8903**	**0.894**	**0.8856**	**0.9362**	**0.9554**
	EPSNR	**18.6074**	**31.2876**	**24.9777**	**32.7617**	**33.2658**	**21.7497**	**31.5938**	**34.3329**
	FSIM	**0.8912**	**0.9466**	**0.9381**	**0.9495**	**0.9832**	**0.9300**	**0.9764**	**0.9883**

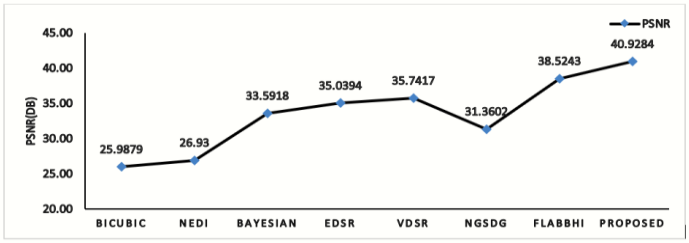

Figure 5a. PSNR values for various dataset using proposed and existing algorithms

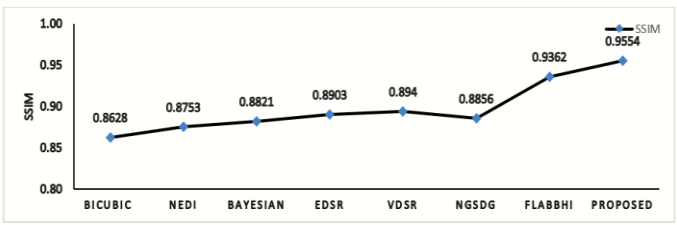

Figure 5b. SSIM values for various dataset using proposed and existing algorithms

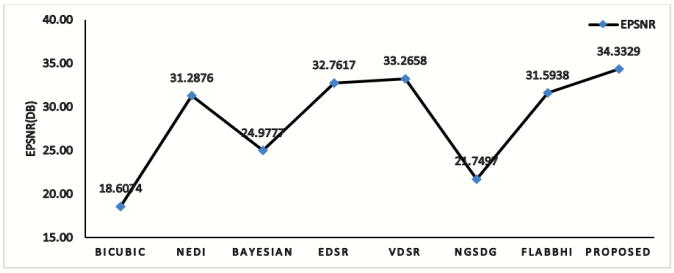

Figure 5c. EPSNR values for various dataset using proposed and existing algorithms

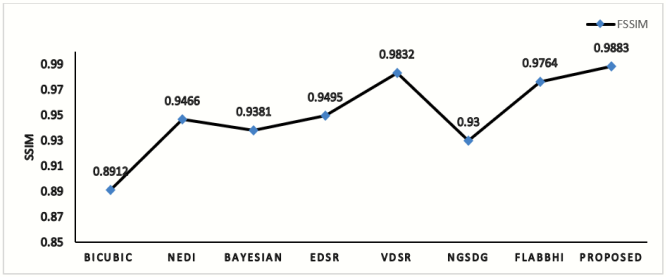

Figure 5d. FSIM values for various dataset using proposed and existing algorithms

V. CONCLUSION

The ANN Quadratic interpolator that was proposed turns out to be superior to the other interpolation methods that are currently in use. Deep learning concepts were used to train, validate, and test the performance of a variety of interpolators, and three distinct datasets—specifically IAPRTC-12, DIV 2K, and CDVS—were employed for these purposes. An analysis of comparable findings demonstrates that the proposed ANN Quadratic interpolator achieves superior outcomes. For each of the three datasets, the average peak signal-to-noise ratio (PSNR) was found to be 40.9742, 40.0176, and 41.8392 respectively. Additionally, the average SSIM was found to be 0.9563, 0.9528, and 0.9571. The average EPSNR was found to be 34.2209, 34.5275, and 34.2503, and the average FSIM was found to be 0.9882, 0.9882, and 0.9885. Hence, the proposed method demonstrates superior quality when measured against other approaches already in use.

REFERENCES

[1] J. Kim, J. K. Lee, and K. M. Lee, "Accurate image super-resolution using very deep convolutional networks," *Proc. IEEE Comput. Soc. Conf. Comput. Vis. Pattern Recognit.*, vol. 2016-Decem, pp. 1646–1654, 2016.

[2] K. W. Hung and W. C. Siu, "Robust soft-decision interpolation using weighted least squares," *IEEE Trans. Image Process.*, vol. 21, no. 3, pp. 1061–1069, 2012.

[3] C. C. Lin, M. H. Sheu, C. Liaw, and H. K. Chiang, "Fast first-order polynomials convolution interpolation for real-time

digital image reconstruction," *IEEE Trans. Circuits Syst. Video Technol.*, vol. 20, no. 9, pp. 1260–1264, 2010.

[4] R. Timofte *et al.*, "NTIRE 2017 Challenge on Single Image Super-Resolution: Methods and Results," *IEEE Comput. Soc. Conf. Comput. Vis. Pattern Recognit. Work.*, vol. 2017-July, pp. 1110–1121, 2017.

[5] C. Ledig *et al.*, "Photo-realistic single image super-resolution using a generative adversarial network," *Proc. - 30th IEEE Conf. Comput. Vis. Pattern Recognition, CVPR 2017*, vol. 2017-Janua, pp. 105–114, 2017.

[6] A. Amanatiadis and I. Andreadis, "A survey on evaluation methods for image interpolation," *Meas. Sci. Technol.*, vol. 20, no. 10, 2009.

[7] Z. Xu, Z. Chen, W. Yi, Q. Gui, W. Hou, and M. Ding, "Deep gradient prior network for DEM super-resolution: Transfer learning from image to DEM," *ISPRS J. Photogramm. Remote Sens.*, vol. 150, no. August 2018, pp. 80–90, 2019.

[8] F. Najar, S. Bourouis, N. Bouguila, and S. Belghith, "Unsupervised learning of finite full covariance multivariate generalized Gaussian mixture models for human activity recognition," *Multimed. Tools Appl.*, vol. 78, no. 13, pp. 18669–18691, 2019.

[9] C. Aguerrebere, A. Almansa, J. Delon, Y. Gousseau, and P. Muse, "A Bayesian Hyperprior Approach for Joint Image Denoising and Interpolation, With an Application to HDR Imaging," *IEEE Trans. Comput. Imaging*, vol. 3, no. 4, pp. 633–646, 2017.

[10] B. Zhong, K. K. Ma, and Z. Lu, "Predictor-corrector image interpolation," *J. Vis. Commun. Image Represent.*, vol. 61, pp. 50–60, 2019.

[11] "Image Interpolation Using Gaussian Mixture Models With Spatially Constrained Patch Clustering, Islamic Azad University , Majlesi Branch , Iran Department of Biomedical Engineering , Isfahan University of Medical Sciences , Iran Sharif University of Technol," no. 91004600, pp. 1613–1617, 2015.

[12] D. F. Noor, Y. Li, Z. Li, S. Bhattacharyya, and G. York, "Multi-Scale Gradient Image Super-Resolution for Preserving SIFT Key Points in Low-Resolution Images," *Signal Process. Image Commun.*, vol. 78, no. November 2018, pp. 236–245, 2019.

[13] K. Chitra and C. Vennila, "A novel patch selection technique in ANN B-Spline Bayesian hyperprior interpolation VLSI architecture using fuzzy logic for highspeed satellite image processing," *J. Ambient Intell. Humaniz. Comput.*, vol. 12, no. 6, pp. 6491–6504, 2021.

[14] V. Chandrasekhar, G. Takacs, M. C. Sam, S. T. Yuriy, R. Grzeszczuk, and B. Girod, "Compressed Histogram of Gradients : A Low-Bitrate Descriptor," pp. 384–399, 2012.

[15] S. P. Mudunuri, S. Sanyal, and S. Biswas, "GenLR-Net: Deep framework for very low resolution face and object recognition with generalization to unseen categories," *IEEE Comput. Soc. Conf. Comput. Vis. Pattern Recognit. Work.*, vol. 2018-June, pp. 602–611, 2018.

[16] B. Lim, S. Son, H. Kim, S. Nah, and K. M. Lee, "Enhanced Deep Residual Networks for Single Image Super-Resolution," *IEEE Comput. Soc. Conf. Comput. Vis. Pattern Recognit. Work.*, vol. 2017-July, pp. 1132–1140, 2017.

[17] X. Wang, K. Yu, C. Dong, X. Tang, and C. C. Loy, "Deep network interpolation for continuous imagery effect transition," *Proc. IEEE Comput. Soc. Conf. Comput. Vis. Pattern Recognit.*, vol. 2019-June, pp. 1692–1701, 2019.

[18] C. Dong, C. C. Loy, K. He, and X. Tang, "Image Super-Resolution Using Deep Convolutional Networks," *IEEE Trans. Pattern Anal. Mach. Intell.*, vol. 38, no. 2, pp. 295–307, 2016.

[19] M. Grubinger, P. Clough, and T. Deselaers, "The IAPR TC-12 Benchmark: A New Evaluation Resource for Visual Information Systems," *Lrec*.

[20] E. Agustsson, "NTIRE 2017 Challenge on Single Image Super-Resolution : Dataset and Study," 2017.

[21] V. R. Chandrasekhar *et al.*, "The stanford mobile visual search data set," *MMSys'11 - Proc. 2011 ACM Multimed. Syst. Conf.*, pp. 117–122, 2011.

[22] J. Xiao, J. Wang, S. Cao, and B. Li, "Application of a Novel and Improved VGG-19 Network in the Detection of Workers Wearing Masks," *J. Phys. Conf. Ser.*, vol. 1518, no. 1, 2020.

[23] Kaiming He et al., "Deep Residual Learning for Image Recognition." In CVPR, 2016."